Macromolecular Research, Vol. 14, No. 4, pp 473-477 (2006)

Notes

The Semi-Transparent Diamond Monochromator at the ESRF Troika Beamlines

Muriel Mattenet*, Oleg Konovalov, and Anders Madsen

European Synchrotron Radiation Facility, 38043 Grenoble, France

Gerhard Grübel

Hasylab/Desy, Notkestrasse 85, 22607 Hamburg, Germany

Received August 11, 2005; Revised February 27, 2006

Introduction

The Troika beamline ID10 at the European Synchrotron Radiation Facility (ESRF) provides a high-brilliance X-ray beam from an undulator source to three experimental stations (ID10A, ID10B and ID10C, Figure 1). When the first monochromator was installed in 1997 the X-ray source was composed of 3 undulators in series installed in the high-straight section 10 of the ESRF storage ring. In details, the source consisted of two U42 undulators (magnet period 42 mm, length 1.6 m) and a mini-gap undulator U26 (26 mm period).

The source size was 928 × 23 μm^2 (H × V) FWHM and the divergence 28× 17 μrad^2 FWHM at 10 keV. An upstream semi-transparent diamond monochromator (Figure 2), located in the ID10 optics hutch, intercepts the undulator beam 28 meters from the source and delivers monochromatic beam to a side-station (ID10B).

The ID10B branch[1] is dedicated to high resolution X-ray diffraction and surface scattering on liquid and solid interfaces comprising grazing-incidence diffraction, grazing-incidence small-angle scattering, and X-ray reflectivity.[2,3]

The beam transmitted through the diamond crystal impinges on a second monochromator located ~44 m downstream the source in the ID10A experimental hutch. This station is dedicated to high resolution WAXS and slow dynamics studies by means of photon correlation spectroscopy with coherent X-rays (XPCS).[4] Applications of XPCS comprise in particular the study of complex fluids including polymer science[5,6] and surface/membrane[7-9] studies.

Through the ID10A monochromator the undulator beam is transmitted to the ID10C end-station. ID10C can operate in white beam conditions (no optics inserted), in "pink beam" conditions (with a mirror monochromator accepting the full undulator harmonic) or with a monochromatic beam delivered by a water-cooled channel-cut Si (111) monochromator. The

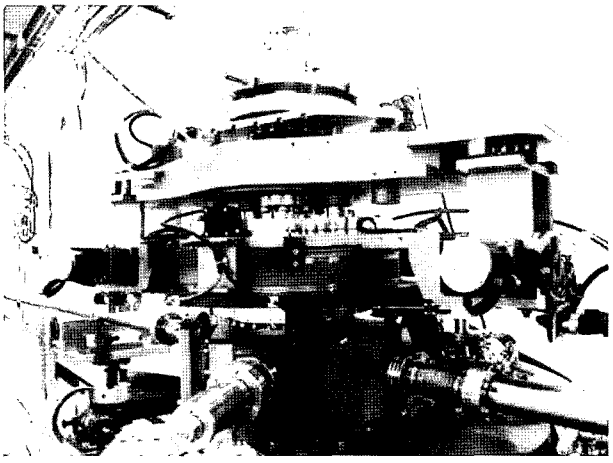

Figure 2. The semi-transparent diamond monochromator installed in the optics hutch of the ESRF Troika beamlines. It provides monochromatic beam to the ID10B side-station.

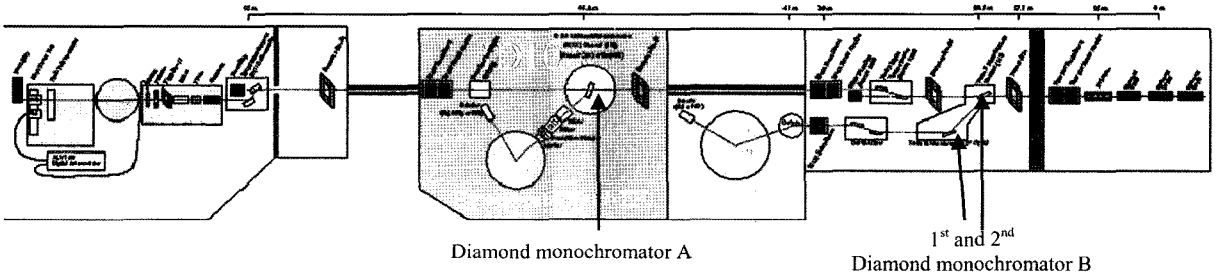

Figure 1. Layout of the Troika Beamlines with the three experimental stations (ID10A, ID10B and ID10C). http://www.esrf.fr/UsersAndScience/Experiments/SCMatter/ID10A/, http://www.esrf.fr/UsersAndScience/Experiments/SCMatter/ID10B/.

*Corresponding Author. E-mail: mattenet@esrf.fr

ID10C end-station is dedicated to SAXS experiments with coherent X-ray beams and XPCS, and experiments with X-ray energies up to 20 keV can be performed.[10]

Beam multiplexing with semi-transparent diamond monochromators has also been realized at the ID14 ESRF macromolecular beamline[11] and is scheduled for the 11A-SWAXS beamline[12] at the Pohang Accelerator Laboratory in Korea.

At Troika the multipurpose character of the satellite stations necessitates a maximum flexibility in terms of resolution, energy tunability and flux, as described in the following.

The Semi-Transparent Diamond Monochromator

Principle. A 120 μm thick diamond (111) crystal intercepts the white undulator beam and Bragg reflects monochromatic radiation to the ID10B station.[13,14] The major part of the spectrum is transmitted through this first diamond to the downstream stations as shown in Figure 3. The spectrum is recorded with a Si(111) crystal in symmetric Bragg geometry at ID10A and the dip at 7971 eV is caused by the Bragg-reflection of the upstream diamond crystal operating at this energy.

Multi-Crystal Holders. The multicrystal monochromator[15] for the ID10A branch is designed to support four X-ray transparent crystals pre-aligned during the mounting to scatter horizontally: i) a (100) diamond allowing reflection from (220) in symmetric Laue geometry, ii) a (100) diamond allowing reflection from (111) in asymmetric Laue geometry, iii) a beryllium crystal allowing reflection from (200) in symmetric Laue geometry, and iv) a Si(111) crystal operating in symmetric Bragg geometry. Figure 4 shows the energy range covered by the different monochromator crystals.

The ID10B branch is also equipped with a multicrystal monochromator. The beam from this monochromator impinges on a second crystal which is offset horizontally by 850 mm to produce a beam traveling parallel to the white-beam. This double-crystal configuration operates optionally with two pairs of either diamond (111) or diamond (220) crystals in symmetric Bragg geometry.

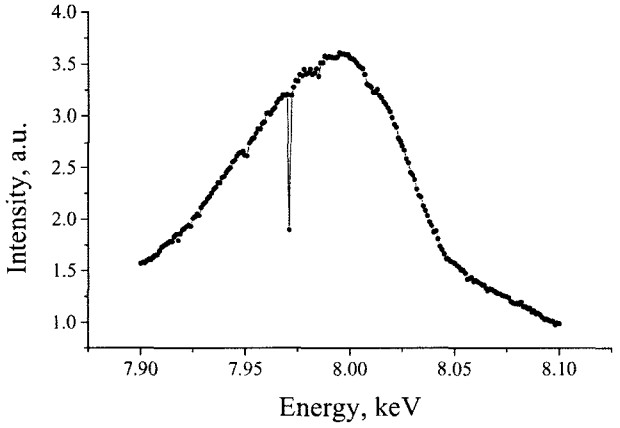

Figure 3. Measured spectrum of the 3rd harmonic of the Troika U42 undulator centered at 8 keV after the 1st diamond monochromator.

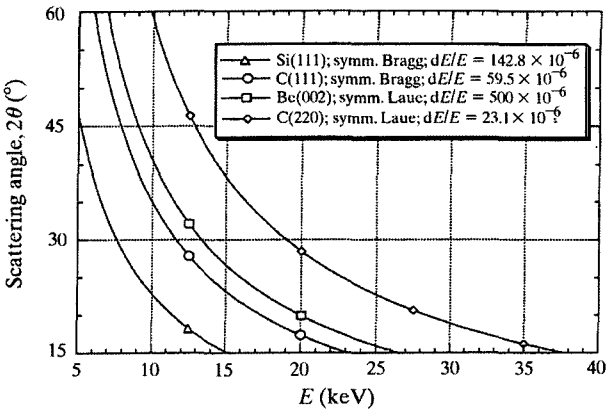

Figure 4. Energy range covered by the multicrystal monochromator at ID10A.

Table I. Technical Specifications of the Monochromator Motions

	Stroke	Resolution
Rotation [degrees]	0 to 45	1×10^{-4}
Tilt [degrees]	-10 to +5	1×10^{-3}
z-motion	50 mm	5 μm
xy-adjustment	±2.5 mm	1 μm

Monochromator Assembly. All monochromator motions are driven from outside the vessel ensuring perfect UHV compatibility. Large external rotations, tilt and translation stages ensure excellent positioning of the centers-of-rotation of the crystals with respect to the beam. The design is simple and a minimum of maintenance is required due to the strict use of commercial motion devices. The monochromator assembly[15] provides high-resolution motion under UHV conditions (10^{-8} mbar) fulfilling the technical specifications given in Table I.

Recent Upgrade of the Troika Undulator Source

In order to provide more photon flux at the sample, the undulators in the ESRF straight section 10 have recently been upgraded. Three new devices are now in place: one U35 (35 mm period), one U27 (27 mm period), and one revolver segment carrying both U35 and U27 undulators. The revolver allows to switch easily between two configurations: either a set of two U35 and one U27 or a set of one U35 and two U27. Preliminary tests with this new source showed that the divergence of the diffracted beam in maximum heat load conditions was increased compared to the previous situation, particularly with the Si monochromator at ID10A. The real impact on the monochromator crystals due to the increased

heat load remains to be definitively evaluated but some basic considerations are made below.

Thermal Environment of the Crystals

Let us consider a Si(111) crystal, 10 mm × 10 mm × 500 μm thick. The integrated absorbed power is given by:

$$P_{abs} = \int I_0(E)(1-e^{-\mu(E)x})dE \quad (1)$$

where $I_0(E)$ and $\mu(E)$ are the energy dependent incident intensity and linear absorption coefficient respectively, and x is the apparent thickness of the crystal.

The power density D is given by: $D[\mathrm{W/m^2}]=P_{abs}/A$ where A is the area of the beam footprint on the crystal. In horizontal Bragg scattering geometry the height of the footprint corresponds to the height of the beam and the length of the footprint equals the projected width of the incident beam. The Bragg angle θ_B is defined as follows:

$$n\lambda = 2d_{hkl}\sin\theta_B \quad (2)$$

where λ[Å]=12.4/E[keV] links the X-ray wavelength λ and the energy E, and d_{hkl} is the lattice spacing for the reflection. The beam size at the position of the diamond monochromator is approximately 1 mm × 0.5 mm (H × V). The integrated power for the old undulator configuration was 123 W and with the recent update of the source, this value is increased to 283 W. Be lenses are often inserted to focus the beam down to a height of 0.05 mm at the ID10A monochromator position. The horizontal width is collimated down to 0.3 mm, thus reducing the absorbed power by a factor of three. In this configuration the integrated thermal power is estimated to 20 W for the first configuration and 46 W for the recent update. The power density for the first configuration was 330 W/mm^2.

The existing crystal cooling scheme is designed in order to minimize the deformation of the crystal surface.[16] The two edges of the crystal are floating on an InGa eutectic layer deposited on its supporting Cu inset. The inset is Ni-coated to avoid diffusion of Ga into Cu. This inset is directly attached to the water cooled crystal support where water flows gently inside to avoid any vibrations. The limitations of the existing cooling scheme are: a restricted cooling area on the crystal, a limited convective heat transfer coefficient of the InGa eutectic (estimated to 10,000 W/m^2.K) and a limited convective heat transfer coefficient of the dry Cu/Cu interface of the insert and the crystal support (estimated to 1,000 to 2,000 W/m^2.K). To overcome these limitations, we propose to increase the effective area of the thermal exchange with the crystal, remove the InGa interface and implement a direct micro channel cooling[17] in the Si thus also avoiding the dry Cu/Cu interface. We envisage to reduce the thickness of the Si crystal as well. A technological solution to fulfill these requirements is to manufacture, based on photolithography, micro channels in a Si substrate and then assemble a normal Si crystal and the machined Si substrate using molecular bonding technology (Figure 5).

The heat power which is absorbed by the diamond crystal is smaller due to the fact that its thickness is three times smaller than that of the Si crystal, and the absorption coefficient for diamond is smaller than for Si. The semi-transparent diamond monochromator of ID10B is in operation since 1998 and no major degradation of the quality of the crystal surface has been observed. The existing cooling scheme using circulating water at 20 °C was suitable for the old undulator configuration. To overcome the increase of heat load caused by the new undulators, we envisage to keep the InGa interface but suppress the dry Cu/Cu interface. The cooling system will then be implemented directly in the diamond crystal support.

Quantitative Estimation of the Contribution of Microfluidics Cooling

The convective heat transfer coefficient h between the water and the crystal is the key parameter which defines the efficiency of the cooling. In micro channels, this convective

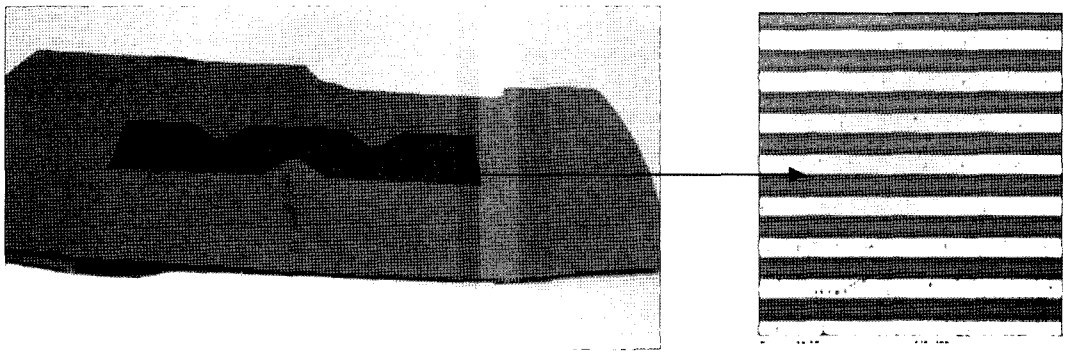

Figure 5. Micro channels are etched in a substrate which is attached by molecular bounding to the crystal (Manufactured by CEA/LETI).

heat transfer coefficient h is given by the Nusselt number N_u and the Reynolds number R_e which characterize the flow regime of the liquid as follows[18]:

$$N_u = \frac{h \cdot D_h}{k_l} \text{ and } R_e = \rho VD/\mu \quad (3)\,(4)$$

where D_h is the equivalent hydraulic diameter [m]. For a rectangular section:

$$D_h = \frac{2Dl_c}{(D+l_c)} \quad (5)$$

k_l is the thermal conductivity of the coolant [W/m^2.K], ρ is the coolant density [kg/m^3], V is the velocity of the coolant [m/s], l_c the width of a channel [m], D is the depth of the channels [m] and μ the dynamic viscosity of the coolant [Kg/s.m].

In the laminar regime,

$$N_u = -14.859 + 65.623G - 71.907G^2 + 29.384G^3 \quad (6)$$

where $G = \frac{(D/l_c)^2+1}{(D/l_c+1)^2}$

When the Prandtl Number P_r, given by $P_r = \mu C_p/k_l$, (where C_p is the heat capacity of the coolant) is between 1.5 and 500 and the Reynolds number is around or above 1,500 for micro channels, we may consider that we are in the turbulent regime. The Nusselt number has then to be calculated from eq. (7).

$$N_u = 0.012(R_e^{0.87} - 280) + P_r^{0.4} \quad (7)$$

Let's consider micro channels with a depth D of 200 μm and a width l_c of 70 μm in the laminar regime. An analytical estimation gives then a value of N_u=5.15 and a value for the convective heat transfer coefficient between the water coolant and the substrate of h=30,000 W/m^2.K. This value is three times better than the value obtained with the InGa eutectic.

Results from the Finite Element Analysis

The thermo-mechanical analysis is based on a multiphysics finite element analysis software (Femlab). The starting point is the behavior of the 500 μm Si(111) crystal under the heat conditions related to the previous undulator configuration. The full vertical beam is focused down to a height of 50 μm and the width is slit down to 0.3 mm. The energy is 8 keV, which gives rise to a footprint of 50 μm in height and 1.24 mm in length along the crystal. The total absorbed power is 20 Watts. The dry Cu/Cu interface is not taken into account because we consider that the contact area is large enough to compensate the poor the thermal contact. The InGa coefficient of convection equals 10,000 W/m^2.K and the contact area on the crystal is 40 mm^2. The thermal conductivity and the expansion coefficient of Si are not taken as constants but are temperature dependent. In such conditions, the maximum temperature on the crystal is 880 K for a coolant at 295 K and the minimum temperature is 338 K. Hence, the temperature gradient over the crystal is 542 K. If we consider the proposed cooling design with 18 micro-channels on

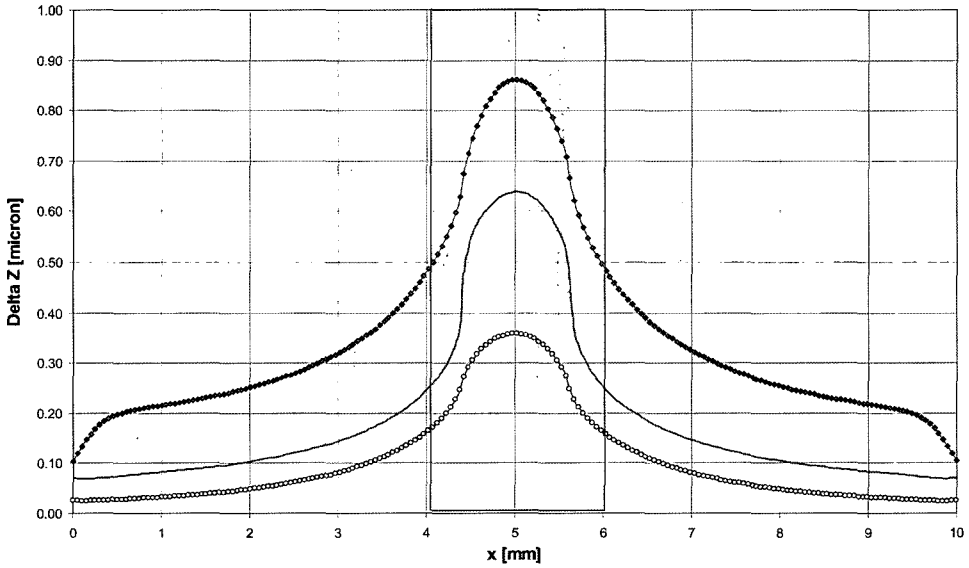

Figure 6. Absorbed power: 20 Watts. Power density: 330 × 10^6 W/m^2. Beam cross section: 0.05 × 0.3 mm^2 (VxH) (vertical focusing). Calculated z deformation of the Si crystal surface along the beam introduced by the X-ray beam in three cases. Diamonds points: present cooling scheme, Continuous line: the micro-channel cooling scheme composed of 9 micro-channels on both side and Open circles: the 18 micro-channels on both sides cooling scheme described in the body text.

both end faces, the maximum temperature drops to 604 K and the minimum temperature to 296 K. Hence, the difference is clearly reduced and equals 308 K.

Figure 6 shows the calculated z deformation of the surface of the crystal along the beam. The amplitude of the deformation under the incident beam (the two central millimeters) in the 18 micro channels configuration, is reduced by more than a factor of two compared to the present cooling scheme. Therefore the crystal is able to support more than twice the thermal load for a similar maximum allowed deformation. Consequently, this new micro channel cooling scheme should minimize the heat load issues introduced by the recent upgrade of undulators at ID10.

Summary

The above described semi-transparent monochromators have been operational since 1997. Four units are permanently operating at the ESRF beamline ID14. Two units are in continuous operation at ID10 and one unit is installed at the APS beamline 8-ID in USA.

The water cooling of the crystals is currently being revised and above we showed that improvements most likely are possible by using microfluidics techniques. Further tests will be performed in collaboration with the CEA-France and tested at ESRF. Parallel developments including nanofluids as coolants are under evaluation. Combination of nanofluidics and microfluidics cooling devices are under study.

The authors are grateful to C. Gillot and J-A. Gruss for useful discussions and advices, and to S.Mcheik for his work on the thermal model.

References

(1) D. Smilgies, N. Boudet, B. Struth, and O. Konovalov, *J. Sync. Rad.*, **12**, 329-339 (2005).
(2) V. M. Kaganer, B. Jenichen, G. Paris, K. H. Ploog, O. Konovalov, and P. Mikulik, *Phys. Rev. B*, **66**, 035310, (2002).
(3) Ph. Fontaine, M. Goldmann, P. Muller, M.-C. Faur, O. Konovalov, and M. P. Krafft, *J. Am. Chem. Soc.*, **127**, 512 (2005).
(4) G. Grübel and F. Zontone, *J. of Alloys and Compounds*, **362**, 3 (2004).
(5) S. G. J. Mochrie, A. M. Mayes, A. R. Sandy, M. Sutton, S. Brauer, G. B. Stephenson, D. L. Abernathy, and G. Grübel, *Phys. Rev. Lett.*, **78**, 1275 (1997).
(6) A. Papagiannopoulos, T. A. Waigh, A. Fluerasu, C. Ferny-hough, and A. Madsen, *J. Phys.: Condens. Matter*, **17**, L279 (2005).
(7) A. Madsen, T. Seydel, M. Sprung, C. Gutt, M. Tolan, and G. Grübel, *Phys. Rev. Lett.*, **92**, 096104 (2004).
(8) A. Madsen, J. Als-Nielsen, and G. Grübel, *Phys. Rev. Lett.*, **90**, 085701 (2003).
(9) I. Sikharulidze, I. P. Dolbnya, A. Fera, A. Madsen, B. I Ostrovskii, and W. H. de Jeu, *Phys. Rev. Lett.*, **88**, 115503 (2002).
(10) T. Thurn-Albrecht, F. Zontone, G. Grübel, W. Steffen, P. Müller-Buschbaum, and A. Patkowski, *Phys. Rev. E*, **68**, 031407 (2003).
(11) http://www.esrf.fr/UsersAndScience/Experiments/MX/ID14-1/.
(12) http://pal.postech.ac.kr/eng/beam/beam.php.
(13) G. Grübel, J. Als-Nielsen, and A. Freund, *J. de Phys.*, **IV**, C9 (1994).
(14) J. Als-Nielsen, A. Freund, G. Grübel *et al.*, *Nucl. Instrum. Methods Phys. Res. B*, **94**, 306 (1994).
(15) M. Mattenet, T. Schneider, and G. Grübel, *J. Sync. Rad.*, **5**, 651 (1998).
(16) M. Mattenet and G. Marot, *SPIE*, **2855**, 180 (1996).
(17) G. P. Celata, *et al.*, *Heat transfer and Transport Phenomena in Microscale*, **Oct.15-20**, 24-31 (2000).
(18) C. Gillot, PhD Thesis, UJF/CEA Grenoble, France (2000).